A High-Resolution FT-IR Study of the Fundamental Bands ν_7, ν_8, and ν_{18} of Ethene Secondary Ozonide

Valdas Sablinskas,*,† Flemming Hegelund,‡ Justinas Ceponkus,† Ruta Bariseviciute,† Valdemaras Aleksa,† and Bengt Nelander§

Department of General Physics and Spectroscopy, Vilnius University, Universiteto street 3, Vilnius-01513, Lithuania, Department of Chemistry, Aarhus University, Langelandsgade 140, DK-8000 Aarhus C, Denmark, and Chemical Center, Department of Chemical Physics, Lund University, P.O. Box 124, S-221 00 Lund, Sweden

Received: April 1, 2005; In Final Form: June 16, 2005

Ozonization reaction of ethene in neat film at 77 K was performed. Separation of ethene secondary ozonide from the other products of the reaction was performed by continuous pumping of the reactor. Only the products, which evaporated from the walls of the reactor at 185 K, were transferred to the gas cell. The high-resolution infrared absorption spectrum of gaseous ethene secondary ozonide ($C_2H_4O_3$) in a static gas long-path absorption cell has been recorded in the 900−1100 cm^{-1} spectral region at 185 K. The spectral resolution was 0.003 cm^{-1}. Analyses of the ν_7(A) band at 1037.0 cm^{-1}, the ν_8(A) band at 956.1 cm^{-1}, and the ν_{18}(B) band at 1082.1 cm^{-1} have been performed using the Watson Hamiltonian model (A, reduction; III^r, representation). A set of ground-state rotational and quartic centrifugal distortion constants have been obtained, and upper state spectroscopic constants have been determined for the bands investigated. A local resonance observed in ν_{18} is explained as c-Coriolis interaction with $\nu_{10} + \nu_{11}$.

1. Introduction

Among organic compounds present in troposphere, the alkenes are unique as they are reactive toward ozone. The currently generally accepted Criege mechanism[1] assumes that the ozonization reaction of alkenes proceeds in three steps: (I) formation of primary ozonide (POZ), (II) decomposition of POZ into a carbonyl compound R−CHO and a carbonyl oxide R−COO, and (III) addition of the carbonyl compound to the carbonyl oxide to form secondary ozonide (SOZ). The intermediate products of the reaction are formed vibrationally excited, and the fate of the reaction very much depends on the possibilities for cooling of these products. Considerable collisional cooling of the intermediate products is needed for the reaction to proceed according to the Criege scheme. SOZ by itself is a labile compound; its stability varies with the size and shape of the radical, attached to the five-membered ring COOCO. Ethene SOZ is the smallest and most unstable member of the alkenes SOZ. In our experiments, this compound nearly completely decomposes at room temperature during 12 h. It is accepted that the Criege mechanism is valid for the ozonization reaction in the condensed phase, but the reaction mechanism in the gaseous phase has still not been established in full detail.[2]

The structure of ethene SOZ ($C_2H_4O_3$) was established in 1972 by Gillies and Kuczkowski[3] from microwave measurements. They showed that the molecular point group is C_2 with the rotational axis coinciding with the *b*-axis of the molecule (Figure 1). The vibrational spectrum of ethene SOZ isolated in a solid-state argon matrix was measured by Kühne and Günthard[4] in 1976, and most of the fundamental bands were assigned. The vibrational assignment was recently modified by Samuni and Haas from their ab initio study of the normal modes of the molecule.[5]

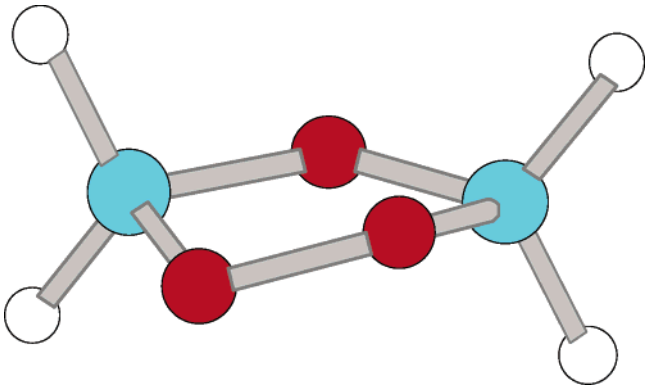

Figure 1. Structure of ethene SOZ.

To our knowledge, no previous high-resolution infrared study has been published for the ethene SOZ in the gas phase. In the present paper, we investigate three fundamental bands in the 950−1100 cm^{-1} region: the weak CO symmetric stretching mode ν_7(A) at 1037 cm^{-1}, the strong COC deformation mode ν_8(A) at 956 cm^{-1}, and the strong asymmetric COC stretching mode ν_{18}(B) at 1082 cm^{-1}. An improved set of ground-state rotational and centrifugal distortion constants is obtained from a simultaneous analysis of our present spectra of ν_8 and ν_{18}, and the ground-state microwave measurements.[3] Upper state spectroscopic constants are obtained from separate fits of the three bands, and a c-Coriolis perturbation observed in ν_{18} is discussed in some detail.

2. Experimental Details

Ozone was prepared from oxygen by electric discharge in a glass reactor cooled by L-N_2. The reactor was filled with 100

* Corresponding author. E-mail: valdas.sablinskas@ff.vu.lt.
† Vilnius University.
‡ Aarhus University.
§ Lund University.

10.1021/jp051647e CCC: $30.25
Published on Web 09/13/2005

Torr L of oxygen and left for 1 h with electrical discharge between electrodes fixed on the inner and outer walls of the reactor. A mixture of ozone and oxygen was trapped on cold walls of the reactor during the discharge. After the discharge was stopped, oxygen was removed by pumping on the reactor for 30 min. The saturated vapor pressure of oxygen at 77 K is much higher than the saturated vapor pressure of ozone, and in this way pure ozone was left in the reactor. Subsequently, ozone was trapped on silica gel, cooled with dry ice.

The ethene SOZ has been prepared by reacting ozone and ethylene in neat film, formed on the wall of the stainless steel reactor at 77 K. Mixtures of ozone and olefins tend to be explosive. To ensure better mixing of ozone with ethylene, the reactants were introduced to the reactor in small portions, not exciding 10 Torr L. This allowed the ozone and ethene to form a sandwich-type structure consisting of consecutively deposited thin films. This multilayer film was formed on a large surface area in the reactor, and any localized build-up of reactants was prevented. Attempts to use bigger portions of reactants produced an explosive decomposition of the reaction mixture. Once the reactants were in the reactor, cooling of the reactor was stopped and the warming process was allowed to begin. Separation of ethene SOZ from the other products of the reaction was performed by continuous pumping of the reactor. Only the products, which evaporated from the walls of the reactor at 185 K, were transferred to multipass IR gas cell, cooled to 185 K.

High-resolution infrared absorption spectra were recorded on the Bruker IFS 120 HR Fourier transform spectrometer at the Swedish national laboratory of synchrotron radiation MAX-laboratory in Lund. The spectra were recorded at 0.003 cm^{-1} spectral resolution. To eliminate radiation >1100 cm^{-1}, a high transmission (T > 90%) 9-μm low pass optical filter was used. For recording of the HR spectra, the globar light source, a KBr beam splitter, and an HgCdTe detector were used.

A 200 L absorption gas cell, made of stainless steel, with White optics, and equipped with CsI windows, was used to obtain the HR spectra. The base length of the cell was 2.85 m. A total number of 24 passes were used for recording of the spectra. The pressure of ethene SOZ in the gas cell was less than 10 Pa. Single-beam spectra were recorded with 0.003 cm^{-1} resolution without zero filling and with boxcar apodization. The background spectrum of the empty cell was recorded at lower resolution, using an appropriate zero filling factor. The final absorbance spectra were free of the periodical interference pattern, which comes from the cell windows and is rather strong in single beam spectra.

3. Assignment of the Bands

Ethene SOZ is a near oblate asymmetric top molecule of C_2 symmetry with $\kappa \approx 0.918$. Eleven of the normal vibrations of the molecule, $\nu_1-\nu_{11}$, are totally symmetric (A). The remaining 10, $\nu_{12}-\nu_{21}$ are of B symmetry in the C_2 point group. The totally symmetric fundamentals give rise to b-type bands for which the strongest transitions are governed by the oblate symmetric top rotational selection rule $\Delta K_c = \pm 1$. The fundamentals of B-symmetry yield a,c-hybrid bands. For the strongest transitions of the a-component, $\Delta K_c = \pm 1$, and for the c-component, $\Delta K_c = 0$.

From the survey spectrum in Figure 2, it is seen that ν_7 and ν_8 appear as typical b-type bands with a minimum of intensity in the band center region. Intense series of ^{P}P- and ^{R}R-branches (i.e., transitions with $\Delta K_c = \Delta J = -1$ and $\Delta K_c = \Delta J = +1$, respectively) dominate the band structure. The individual lines in the series are spaced A + B $\approx$ 0.545 cm^{-1}, and it is easy to pick out the series. Also, the series start (i.e., for $J = K_c$) is straightforward to locate because this is the most intense line in the series. In Figure 3, the assignment of a small part of the R-wing of ν_8 is shown. The strongest transitions $^{R}R_K(K)$ are easy to identify. There is also a tendency of clustering for lines with the same value for $2J - K_c$. This is because the molecule is nearly planar, that is, A $\approx$ B $\approx$ 2C. Near the band center region of ν_8, a number of ^{R}Q- and ^{P}Q-branch series are seen. Figure 4 shows the assignment to J and K_c of a part of the ^{R}Q-branch. In the weak ν_7 band, we were not able to establish convincing Q-branch assignments.

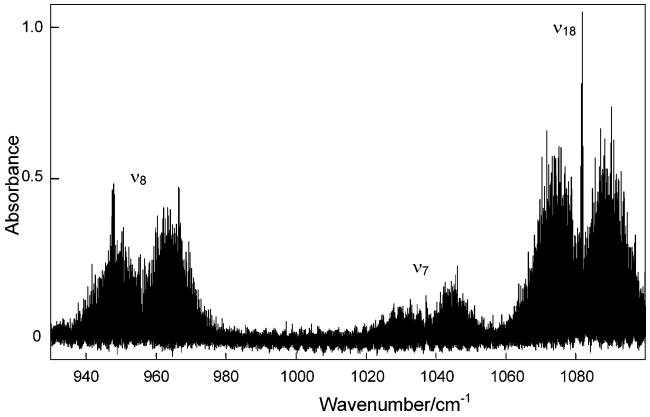

Figure 2. HR FTIR absorption spectrum of ethene SOZ in spectral region of ν_7, ν_8, and ν_{18} fundamental vibrations.

As seen in Figure 2, a strong Q-branch appears near the band center of ν_{18}. Such a structure, which is not well resolved even under high resolution, indicates a,c-band type. The rotational fine structure in the P- and R-wing of ν_{18} is similar to that of b-type bands with series spaced ca. 0.545 cm^{-1}, each showing a clear series start. Also, a tendency of clustering is clearly seen. This appearance is typical both for a- and for b-type bands, and we therefore conclude that ν_{18} is dominated by its a-component. This is further confirmed by our assignment of weaker ^{R}Q- and ^{P}Q-branch transitions. We have not been able to assign c-type transitions in this band. In Figure 5a, small part of the ^{P}P-branch assignment is shown and cluster structure is indicated for $2J - K_c = 30-32$.

In our assignment procedure of the bands observed, we made systematic use of ground-state combination differences (GSCDs). The rotational ground-state constants from ref 3 were used to predict GSCDs of the type $^{R}R_{K-1}(J-1) - {}^{P}P_{K+1}(J+1)$, which made possible the assignment of individual rotational lines in the observed series to J and K_c. Also, Q- and P,R-branch assignments were checked against each other by GSCDs. To speed up and to complete the process of assignment, we used a semiautomatic procedure based on computer-assisted Loomis−Wood diagrams. These diagrams, which are based on our peak lists, are ordered according to upper state quantum numbers and take into account the GSCDs as originally suggested by Nakagawa and Overend.[6] The assignment and additional fit programs have been developed at Aarhus University.

Some details concerning the assignments of the fundamental bands studied in the present work are summarized in Table 1. About 1600 lines were assigned for ν_8, and ca. one-half that number were assigned for ν_7 and ν_{18}. Short asymmetry split series were assigned for low K_c, typically for $K_c < 5$.

4. Results

4a. Ground-State Analysis. The vibrational ground state of ethene SOZ was studied by microwave spectroscopy,[3] and the

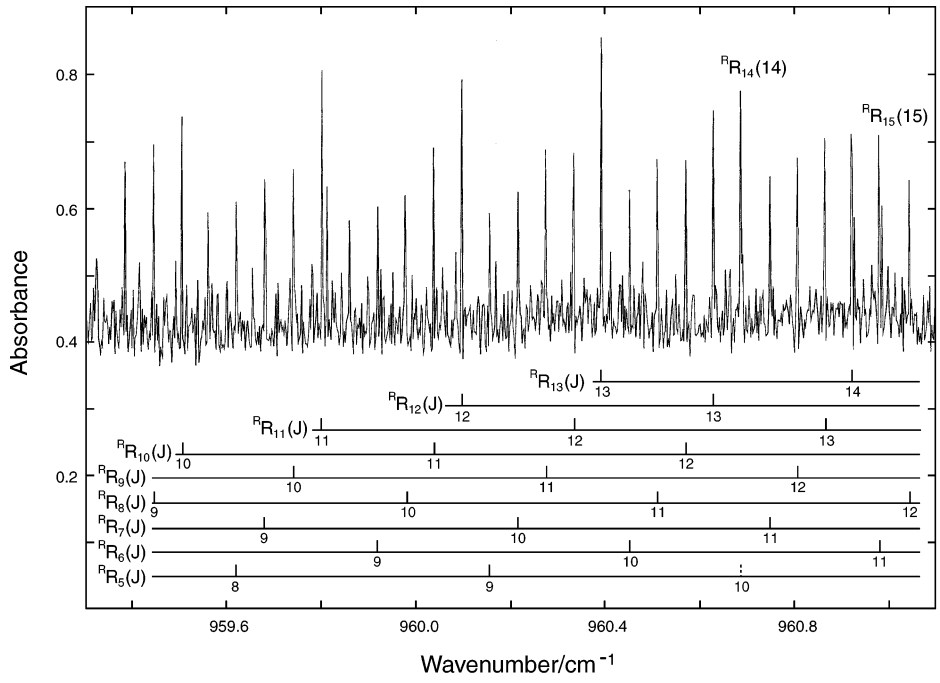

Fig. 3

Figure 3. A close-up on the infrared absorbance spectrum of the R-wing of the ν_8 band of ethene SOZ. The figure shows the *J*-assignment of part of the $^{R}R_5$- to the $^{R}R_{15}$-branches.

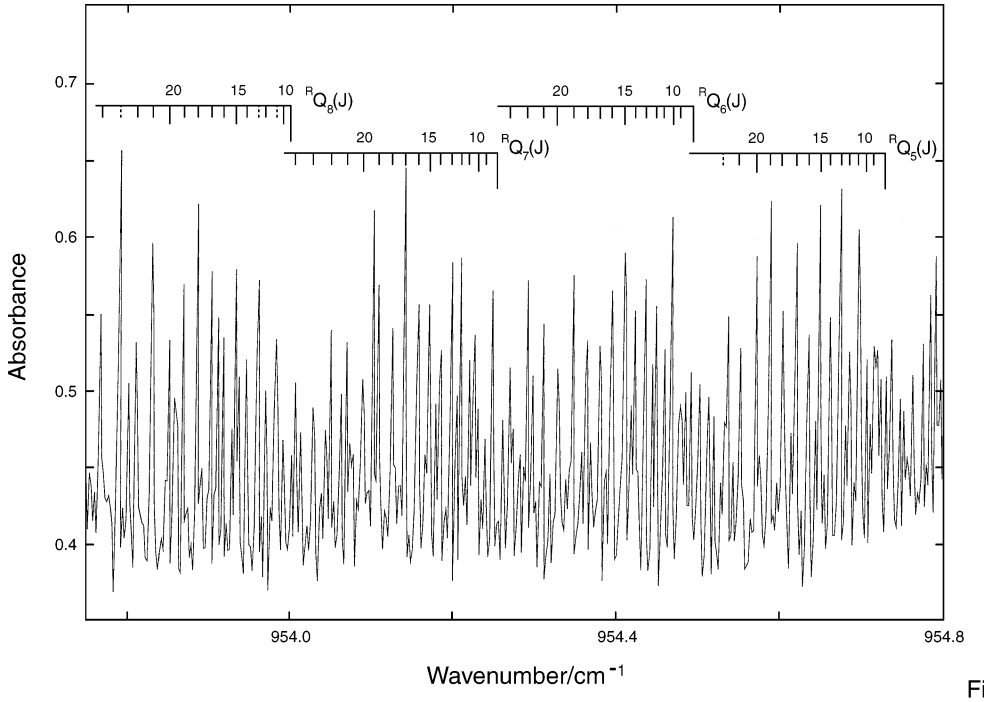

Fig. 4

Figure 4. A small portion of the central part of the infrared absorbance spectrum of the ν_8 band of ethene SOZ. The figure shows the *J*-assignment of the $^{R}Q_5$- to the $^{R}Q_8$-branches.

rotational ground-state constants were obtained; see Table 2, column I. We have redetermined the ground-state parameters for the molecule using our present infrared measurements. Because the ν_7 band is relatively weak, we only fitted GSCDs obtained from the strong ν_8 and ν_{18} bands. Both ν_7 and ν_8 are b-type bands giving GSCDs of the same type, which makes ν_7 less important for a ground-state analysis. A total of 1325 GSCDs mainly based on unblended lines were selected from ν_8 and ν_{18} for our ground-state fit. The Watson Hamiltonian (A, reduction; III^r, representation) was employed including all five quartic centrifugal distortion constants.[7] In column II of Table 2, the ground-state constants obtained are given. Besides the rotational constants, three of the quartic centrifugal distortion constants Δ_J, Δ_{JK}, and Δ_K have been determined for the first time. The two nondiagonal quartic distortion constants δ_J and δ_K could not be obtained significantly from our data. The standard deviation of the fit is 0.00059 cm^{-1}, and the numerical values of the residuals are well below 0.00180 cm^{-1}. The rotational constants obtained agree well with those from the microwave analysis[3] (column I). The largest deviation, which corresponds to ca. four standard errors, is for the A-rotational constant.

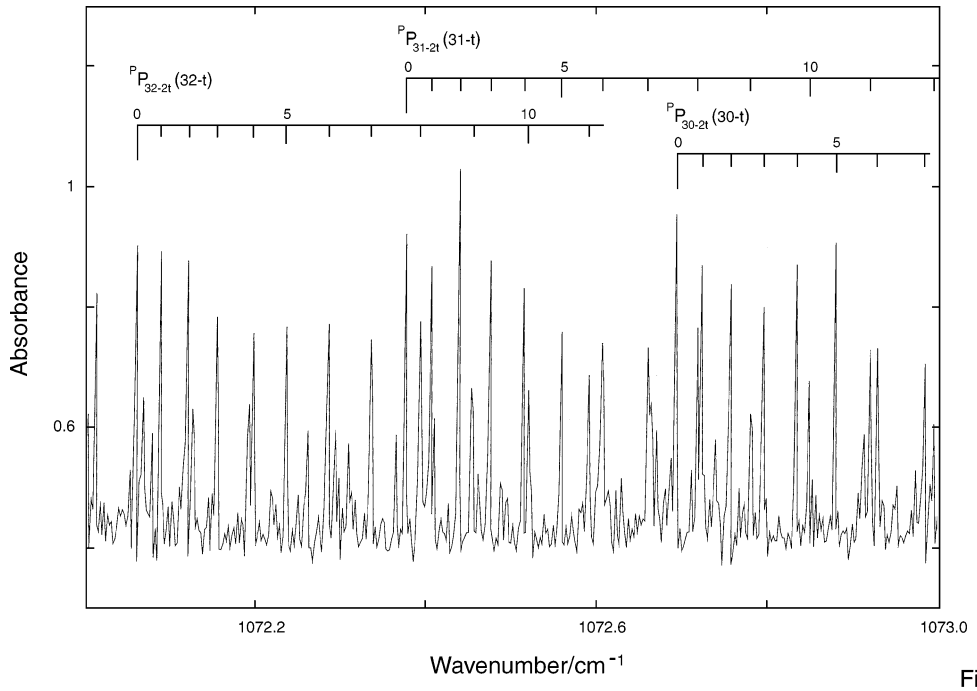

Fig. 5

Figure 5. A close-up on the infrared absorbance spectrum of the P-wing of the ν_{18} band of ethene SOZ. The figure shows clustering around the leading $^{P}P_K(K)$ lines for $K_c = 30-32$.

TABLE 1: Details of Assignment

band	band type	range of assignments	local crossings
ν_7(A; 1037.0 cm^{-1})	b, CO sym. stretch	$1 < K_c < 50$, $J < 53$	
ν_8(A; 956.1 cm^{-1})	b, COC deformation	$K_c < 54$, $J < 58$	$K_c = 33$
ν_{18}(B; 1082.1 cm^{-1})	a, COC asym. stretch	$1 < K_c < 47$, $J < 49$	$K_c = 22,23$

TABLE 2: Ground-State Constants in cm^{-1} for Ethene Secondary Ozonide (A, Reduction; III^r, Representation)

	I[a]	II[b]	III[c]
A	0.27498490(67)[d]	0.2749785(15)	0.27498377(73)
B	0.26998011(67)	0.2699828(15)	0.26998325(73)
C	0.15293046(33)	0.15293094(52)	0.15293079(31)
$\Delta_J \times 10^6$		0.1072(13)	0.1093(8)
$\Delta_{JK} \times 10^6$		−0.1395(33)	−0.1437(22)
$\Delta_K \times 10^7$		0.580(20)	0.601(15)
N[e]	10	1325	1335
σ[f]		0.00059	

[a] **I**, rotational ground-state constants obtained in the MW study; ref 3. [b] **II**, ground-state rotational and centrifugal distortion constants determined from a combined fit of the present GSCDs from ν_8 and ν_{18}. [c] **III**, ground-state rotational and centrifugal distortion constants determined from a combined fit of 10 MW measurements[3] and the GSCDs from ν_8 and ν_{18}. [d] Uncertainties quoted are one standard error. [e] Number of observations in fit. [f] Standard deviation of fit, cm^{-1}.

We have also fitted our present GSCDs simultaneously with the microwave transitions from ref 3. This added 10 observations. In this fit, we gave the microwave data a weight of 10^4 relative to our infrared GSCDs to take into account that the accuracy of the microwave frequencies is higher by a factor of ca. 100 as compared to our infrared wavenumbers. The constants from this fit are given in column III of Table 2. As expected, the inclusion of the microwave data increases the precision of the ground-state parameters, in particular, the rotational constants. The constants from the two fits (columns II and III) agree within ca. three standard errors. A comparison with the microwave values (column I) shows a slightly higher deviation for the B-rotational constant, around four standard errors. We consider the ground-state constants in column III as the best.

TABLE 3: Upper State Constants in cm^{-1} for the ν_7, ν_8, and ν_{18} Bands of Ethene Secondary Ozonide (A, Reduction; III^r, Representation)

	ν_7	ν_8	ν_{18}
ν_0	1037.01111(5)[a]	956.06748(4)	1082.11501(5)
A	0.2740553(100)	0.27482647(37)	0.2744217(31)
B	0.2693487(100)	0.26922995(37)	0.2685297(31)
C	0.15252428(13)	0.15256281(8)	0.15285078(27)
$\Delta_J \times 10^6$	0.10530(29)	0.11527(16)	0.10105(41)
$\Delta_{JK} \times 10^6$	−0.1332(7)	−0.16332(34)	−0.1398(9)
$\Delta_K \times 10^7$	0.5183(41)	0.7701(20)	1.075(7)
$\Phi_K \times 10^{11}$			−0.627(14)
$\delta_J \times 10^8$		0.379(15)	
N[b]	706	1548	787
σ[c]	0.00048	0.00053	0.00051

[a] Uncertainties quoted are one standard error. [b] Number of observations in fit. [c] Standard deviation of fit, cm^{-1}.

4b. Upper State Analysis. To fit the assigned transition wavenumbers in a band and to obtain upper state spectroscopic parameters, we used the asymmetric rotor Hamiltonian of Watson (A, reduction; III^r, representation).[7] In the fit, the observed wavenumbers are converted to upper state energies by addition of the proper ground-state energies, as calculated from the set of ground-state constants given in column III of Table 2. Thus, our fits are on upper state energies. No weighting of the observed transitions is used in the fits.

Table 3 summarizes the upper state constants obtained from the fits of ν_7, ν_8, and ν_{18}. The standard deviations of the fits are around 0.00050 cm^{-1}, which is ca. twice our estimated wavenumber accuracy. In the fits, the band center, the rotational constants, and the three quartic centrifugal distortion constants Δ_J, Δ_{JK}, and Δ_K have been determined for the upper states.

For the ν_{18} band, it was also necessary to include the sextic distortion constants Φ_K to obtain a good fit. As seen from Table 3, Φ_K is obtained negative, and a comparison of Δ_K with its ground-state value (Table 2) reveals that this constant is considerably larger than its ground-state value, $\Delta\Delta_K = 0.472(17) \times 10^{-7}\text{cm}^{-1}$. This indicates the presence of a global c-Coriolis resonance lowering the K_c-levels of ν_{18}. Thus, the perturbing level is of higher vibrational energy than ν_{18}. In addition, a local resonance is observed for $K_c = 22$, 23. The effect of this resonance increases with J, giving rise to negative residuals for $K_c = 22$ and positive residuals for $K_c = 23$. This means that a crossing is present for which the perturbing level is above the $K_c = 22$ level in ν_{18} and below the $K_c = 23$ level in ν_{18}. The observed sense of residuals indicates that the perturber, producing crossing in ν_{18}, also has higher vibrational energy than ν_{18}. Because the selection rules for c-Coriolis resonance are $\Delta K_c = 0, \pm 2, \pm 4$, we suggest that the resonances described above are due the same perturber, giving rise to global c-Coriolis interaction ($\Delta K_c = 0$) as well as local c-Coriolis interaction for $K_c = 22$, 23 ($\Delta K_c = \pm 2$). Assuming ground-state values for the rotational constants of the perturber, we may estimate the vibrational band center of the perturber to be located 11.3(3) cm^{-1} above the band center of ν_{18} from the position of crossing observed in ν_{18}. By symmetry, the perturber is predicted to be of A-symmetry in the C_2 group. Experimental band center values for fundamental levels from solid-state infrared measurements are given in ref 5. From these values, we may suggest that the perturber is the binary combination of the ring deformation vibration ν_{10} and the ring puckering vibration ν_{11}, $\nu_{10} + \nu_{11}$(A), which is predicted at 1089 cm^{-1} from the data in ref 4 neglecting anharmonicity. Our gas-phase study of ν_{18} locates $\nu_{10} + \nu_{11}$ at 1093.4(3) cm^{-1} from the observed effect of local c-Coriolis perturbation. The agreement is reasonable taking into account that the measurements[4] are for the solid state. The c-Coriolis resonance might transfer intensity from ν_{18} to the $\nu_{10} + \nu_{11}$ band. However, we have not been able to assign with confidence line series belonging to this combination band. The upper state constants summarized in Table 3 have been obtained from a fit leaving out 75 perturbed transitions of ν_{18} in the region of crossing.

In our analysis of the ν_8 band, we observed a minor local J-dependent resonance in the $K_c = 33$ level. The observed sense of the residuals indicates that the perturber is located above the $K_c = 33$ level. The neighboring K_c levels seem to be unperturbed, and in our fit only eight transitions for $K_c = 33$ had to be omitted. We have not been able to identify the perturber in this case. As seen from Table 3, a significant value for the quartic centrifugal distortion constant δ_J may be determined. This is certainly because we have been able to trace the typical b-band series of low-K_c P- and R-branch transitions (in particular for $K_c = 0$ and 1 ($K_a + K_c = J + 1$)) out to $J \approx 40$. For the weak ν_7 band, no perturbation seems to be present.

A list of the assigned observed transitions used in the fits described above may be obtained from F.H. or V.S.

5. Summary

In the present paper, we report the first recording of the high-resolution spectra of ethene SOZ in the gas phase. Three bands, ν_7, ν_8, and ν_{18}, in the 950−1100 cm^{-1} region have been assigned and analyzed. From a simultaneous fit of ν_8, ν_{18} and the microwave measurements by Gillies and Kuczkowski,[3] we obtain improved values of the ground-state rotational constants, and three of the quartic centrifugal distortion constants Δ_J, Δ_{JK}, and Δ_K are determined for the first time. Upper state spectroscopic constants including band centers, rotational constants, and quartic centrifugal distortion constants have been obtained for the three bands studied. From a local resonance observed in ν_{18}, we may locate the binary combination level $\nu_{10} + \nu_{11}$ at 1093.4(3) cm^{-1} assuming higher order c-Coriolis perturbation.

Acknowledgment. The running costs of the infrared beam line at the Max laboratory were covered by the Swedish National Science Council. Experiments at Max laboratory of V.S., J.C., R.B., and V.A. were supported partly by the European Community − Research Infrastructure Action under the FP6 "Structuring the European Research Area" Program (through the Integrated Infrastructure Initiative "Integrating Activity on Synchrotron and Free Electron Laser Science") and partly by Nordic Network of Chemical kinetics.

References and Notes

(1) Criegee, R. *Angew. Chem.* **1975**, *87*, 765−771.
(2) Horie, O.; Neeb, P.; Moortgat, G. K. *Int. J. Chem. Kinet.* **1997**, *29*, 461−468.
(3) Gillies, C. V.; Kuczkowski, R. L. *J. Am. Chem. Soc.* **1972**, *94*, 6337−6343.
(4) Kühne, H.; Günthard, Hs. H. *J. Phys. Chem.* **1976**, *80*, 1238−1247.
(5) Samuni, U.; Haas, Y. *Spectrochim. Acta* **1996**, *A52*, 1479−1492.
(6) Nakagawa, T.; Overend, J. *J. Mol. Spectrosc.* **1974**, *50*, 333−348.
(7) Watson, J. K. G. In *Vibrational Spectra and Structure*; Durig, J., Ed.; Elsevier: Amsterdam, 1977; pp 1−89.